CHAPTER III

EXPERIMENT

3.1 TENSILE TEST

3.1.1 SPECIMEN PREPARATION

Three kinds of low-carbon steel sheets (as shown in Table 3-1) for food-can application were selected for the uniaxial tensile test.

Table 3-1 Black Plate (TMBP = Tin Mill Black Plate)

Specimen	Thickness (mm)	Temper Designation	Rockwell Hardness HR30T
A	0.18	DR-8CA	73±3
B	0.20	T-4CA	61±3
C	0.22	T-3	57±3

The term DR means the low-carbon steel sheet coated with tin and the uncoated steel base thereof, respectively. And the steel base has received a second major cold reduction following annealing. The annealing method involves the batch annealing and continuous annealing. In the case that continuous annealing process is selected, the letter CA shall be suffixed to the temper designation.

Table 3-2 lists the chemical composition for the each kind of steel sheet.

3.1.2 DIMENSION OF TEST SPECIMEN

The "dog bone"-shaped test specimens were prepared as the standard sheet-type specimen (ANSI/ASTM A 370 - 77) shown in Fig.3-1.

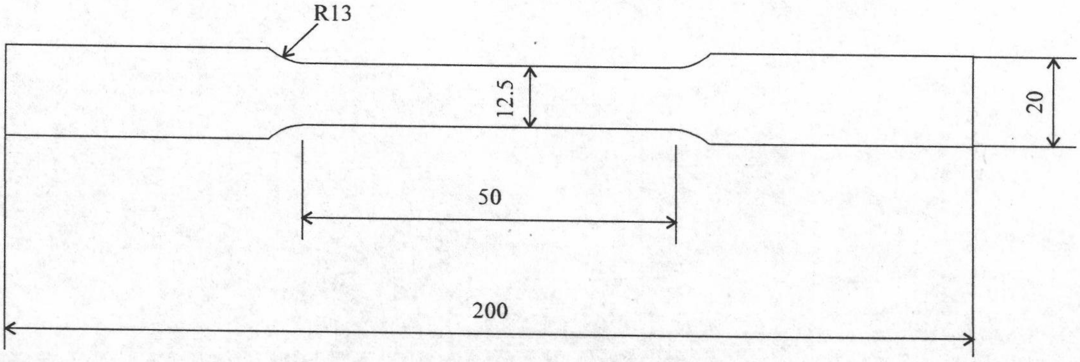

Unit: mm

Fig.3-1 Rectangular tension test specimen

This type of specimen is used for testing metallic materials in the form of sheet.

3.1.3 EQUIPMENT

The tensile test specimens were prepared by using a set of press die with the 0.005 mm clearance. The die used for preparing the specimens is shown in Fig.3-2.

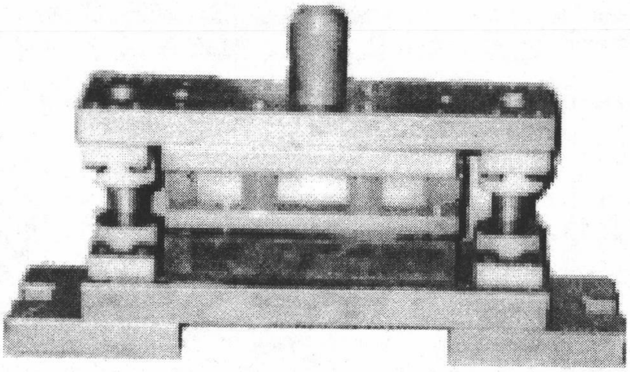

Fig.3-2 Die for preparing tensile specimen.

A mechanical press (60 ton) with a flywheel-type drive was used with the above die to prepare the specimen for the uniaxial tensile test (shown in Fig.3-3).

Table 3-2 Chemical composition of specimen

Specimen	%C	%N	%Al	%Si	%P	%S	%V	%Mn	%Cr	%Ni	%Sn	%Nb	%Ti
A	.0546	.0064	.0601	.005	.0129	.0068	.0022	.2625	.0308	.005	.0023	.0011	.001
B	.0442	.0060	.0592	.0093	.0116	.0027	.0018	.2670	.0274	.0194	.0020	.0010	.001
C	.0792	.0046	.0483	.005	.0153	.0066	.0026	.520	.0314	.005	.0023	.0010	.001

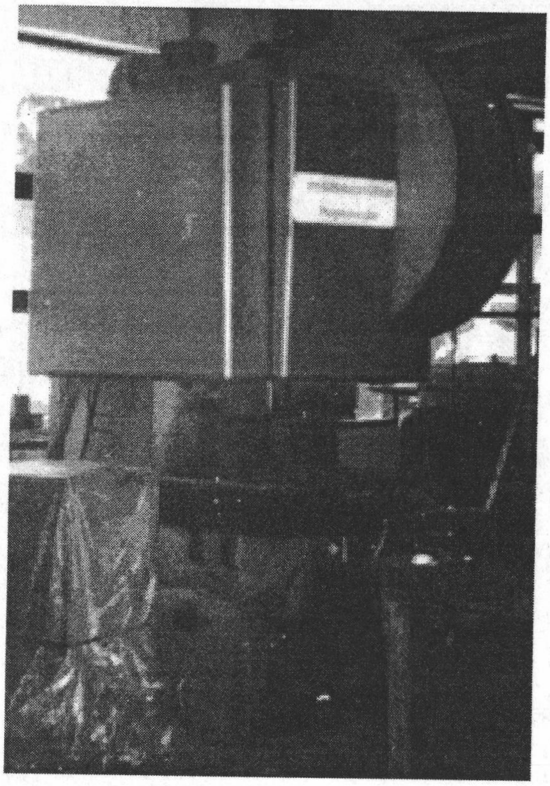

Fig.3-3 60 ton flywheel-type mechanical press

3.1.4 POSITION OF SPECIMEN TAKEN FROM SHEET MATERIAL

During the rolling process which is used to produce metals in sheet form and subsequent annealing, the grains and any inclusions present become elongated in the rolling direction, and a preferred crystallographic orientation developed. This causes a variation of properties with direction. Thus, it is common practice to test specimens cut parallel to the rolling direction and at 45° and 90° to this direction. These are known as longitudinal, diagonal, and transverse specimens, respectively.

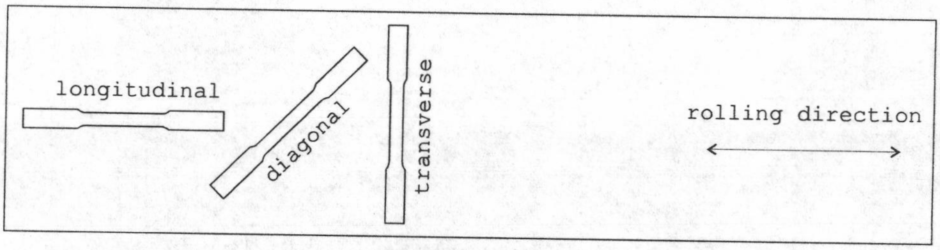

Fig.3-4 Position of samples

3.1.5 GRID PATTERN

For strain analysis, the pattern of circles (10 mm in diameter) was used to make grids on the surfaces of metal sheets (shown in Fig.3-5) to illustrate how the metal moved during the tests. The ink was painted on the stencil (shown in Fig.3-6) which was pressed on the surface of steel sheet. The ink gone through only perforations area of the stencil to contact the steel and completed grid application. The grid pattern allowed direct R-value determination and measurement of stress-strain data somewhat beyond uniform elongation.

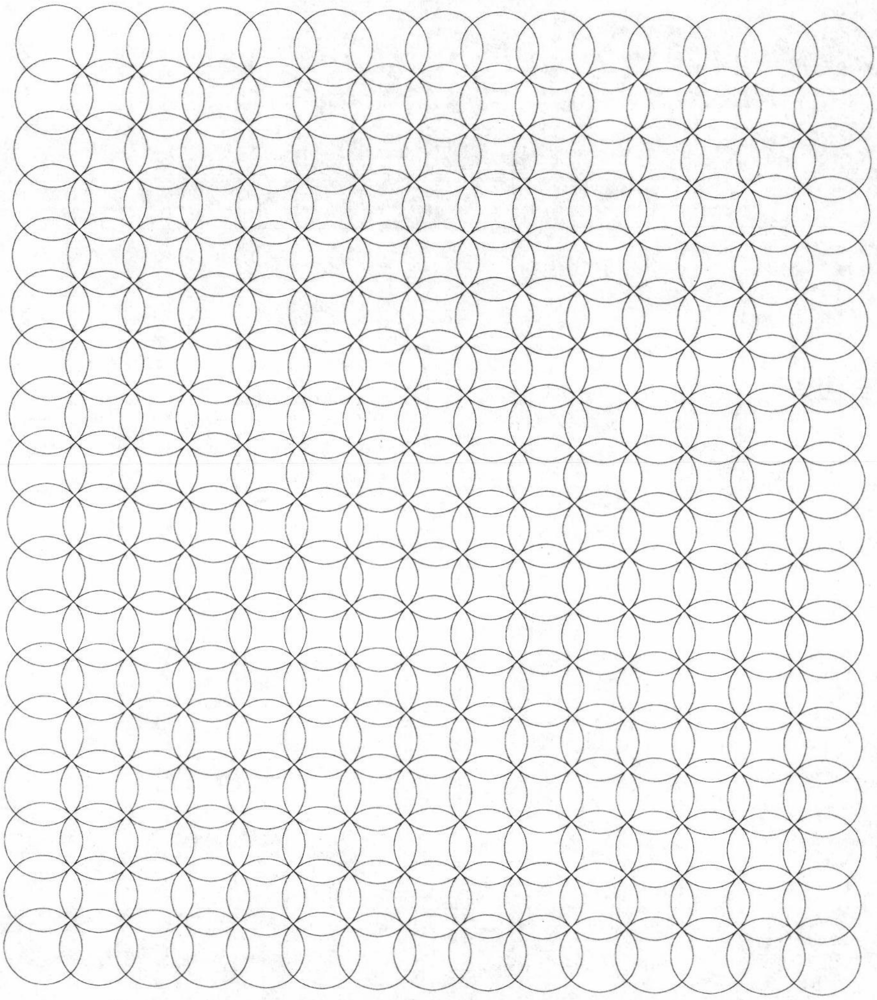

Fig.3-5 Pattern of gage marks for determining strain or scribed circle

Fig.3-6 Ink and screen for preparing grid pattern

3.1.6 APPARATUS

The universal tensile tester was used for tensile tests. The model AG-10 TE mechanical-testing machine can give varieties of testing such as tension, compression, bending, torsion and fatigue tests. The machine cooperates screw-driven system with an electronic controller allows slow testing rate, data collection and data calculation possible.

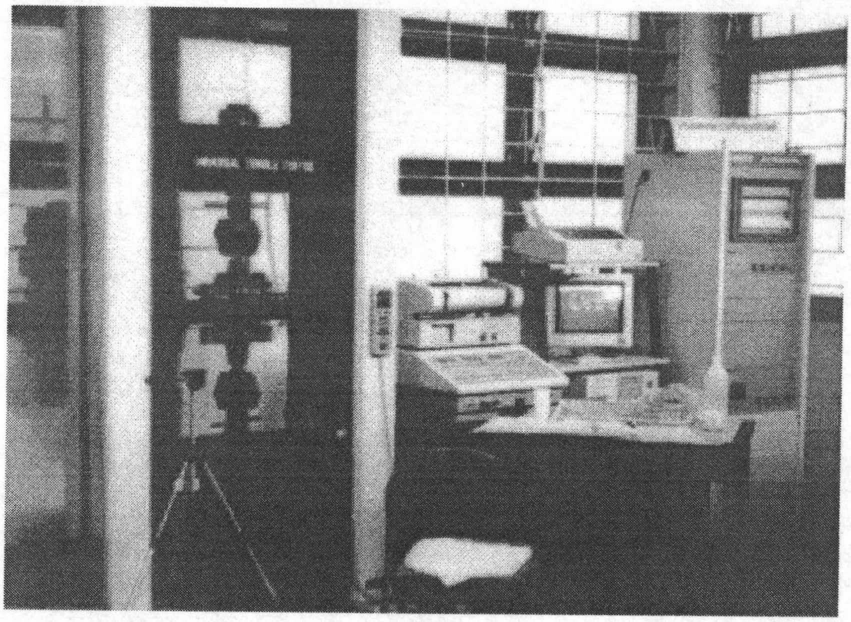

Fig.3-7 Universal tensile tester (AG-10 TE,10 ton)

3.1.7 PROCEDURE

For accurate and reproducible results, uniaxial tensile testing must be performed in a carefully controlled manner.

Measurement of R. Although the R-value is defined as the ratio of width-to-thickness strains, the thickness strain, ε_t, can not be accurately measured in a thin sheet. Therefore the thickness strain is usually found from measurements of length and width strains using volume constancy, $\varepsilon_t=-(\varepsilon_l+\varepsilon_w)$. In this study, the values of ε_l and ε_w were calculated

In this study, the values of ε_l and ε_w were calculated from elongation data by measuring the change of the grid pattern.

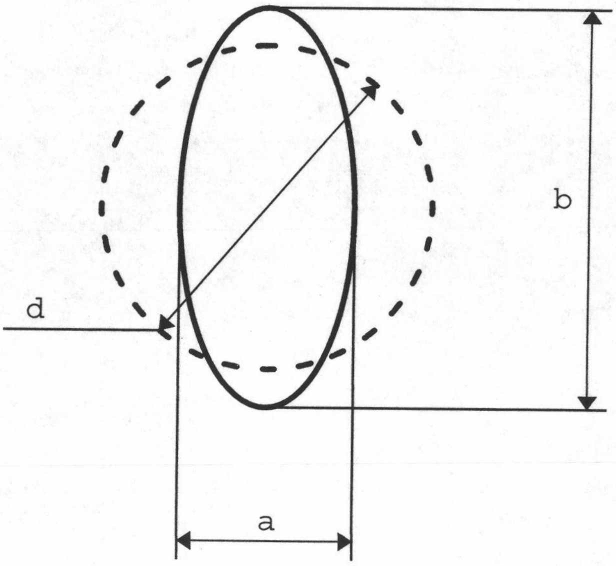

Fig.3-8 Grid pattern for measuring R

As shown in Fig.3-8, $\varepsilon_w=\ln(a/d)$, $\varepsilon_t=\ln(t/t_0)=\ln(d^2/ab)$ where constancy of volume $(4\pi d^2 t_0=4\pi abt)$ had been used and $R=\varepsilon_w/\varepsilon_t=\ln(a/d)/\ln(d^2/ab)$.

Generally, the R value depends on the elongation at which it is measured. It usually measures at 10%, 15% or 20% elongation. In this study, for specimen A, the R-value was measured at 3%

elongation, and 10% elongation for specimen B and specimen C.

Rate of Testing. In this study, the tensile tests were performed on tensile machine at two crosshead rates: 10^{-3} mm/s and 5×10^{-3} mm/s. The strain rate is defined as the increase in length per unit length per second. The specimens were tested under these two strain rate, and the testing data received from each strain rate were averaged and analysed. The

Table 3-3 Number of specimen

Tensile axis	Rate 1 10^{-3} mm/s	Rate 2 5×10^{-3} mm/s	Total (PCs)
R.D.	10	10	20
T.D.	10	10	20
45°	10	10	20
Total (PCs)	30	30	60

R.D. - Rolling Direction

T.D. - Transverse Direction

45° - Angle to the rolling direction

quantity of the specimen required for the tensile test was shown in Table 3-3.

3.1.8 RESULTS

A full presentation of the experimental data can not be made because of large numbers. These experiments resulted in more than 5,000 grid readings and the results must, therefore, appear in condensed form. Fig.3-9 shows the stress-strain curve for the specimen A (t = 0.18 mm, longitudinal).

The tensile properties were calculated from the collected data and listed in the Table 3-4. In this table, all plastic properties were averaged by the rule: $X=(1/4)(X_0 + X_{90} + 2X_{45})$ (R.H.Wagoner,1980), where: X_0-property of steel sheet in rolling direction, and X_{90}-property of steel sheet in transverse direction, X_{45}-property of steel sheet in diagonal direction.

I 16894698

Table 3-4 Typical tensile properties of steel sheet specimen A

Tensile axis	Young's modulus GPa	Yield strength MPa	Tensile strength MPa	Uniform elongation %	Total elongation %	Strain-rate sensitivity m	Anisotropy R
R.D.	210	484.36	609.72	4.420	4.937	0.0109	1.43
T.D.	205	483.91	609.19	4.383	4.907	0.0115	1.44
45°	206	485.54	616.93	4.510	5.032	0.0111	1.44
Average	206.8	484.84	613.19	4.456	4.977	0.0112	1.44

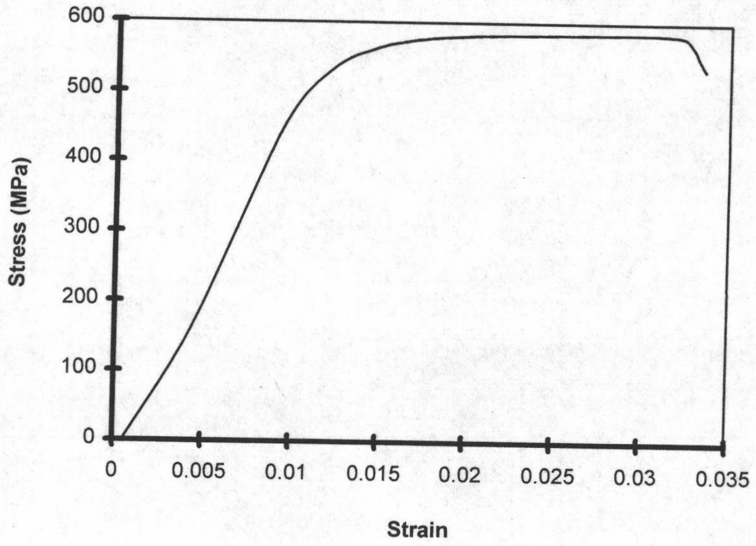

Fig.3-9 Stress-strain curve for specimen A (longitudinal)

Fig.3-10 shows the true stress-true strain data of specimen A (longitudinal) on logarithmic coordinates. With logarithmic coordinates, there is no zero-zero starting point, so the elastic region must start at some finite value. In this figure, the elastic zone near to the transition point and the plastic zone were plotted on logarithmic coordinates. The slope of line for the plastic zone defines the strain-hardening exponent, n, and the intersection of this line with unit strain gives the stress value that defines the magnitude of K, it is often called the strength coefficient.

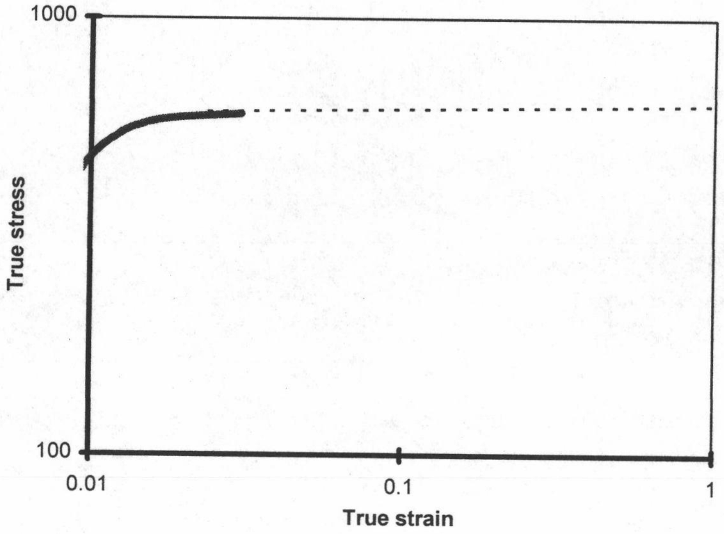

Fig.3-10 True stress-true strain curve for specimen A (longitudinal)

The strain-hardening data was calculated using the method shown in Fig.3-10 and listed in Table 3-5.

The other two kinds of steel sheet were tested in the much same way as the specimen A (longitudinal), and the results are shown below.

Table 3-5 Strain-hardening data of specimen A

Tensile axis	Strength coefficient K (MPa)	Strain-hardening exponent n
R.D.	693	0.048
T.D.	694	0.053
45°	691	0.052
Average	692.3	0.0513

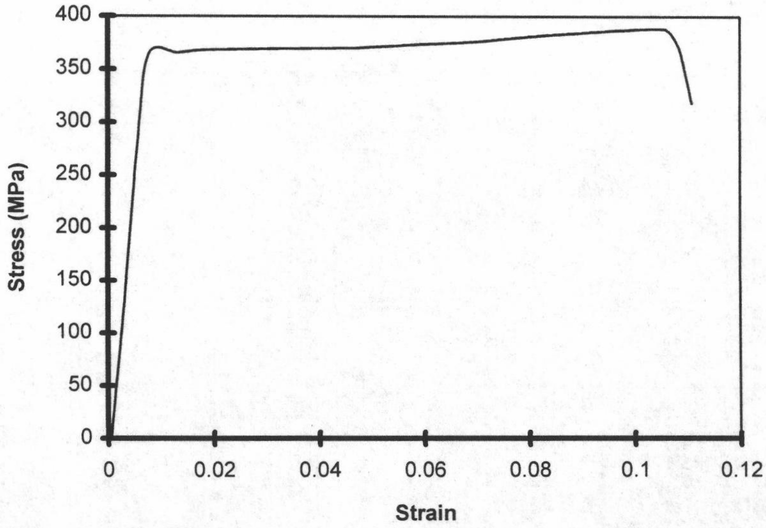

Fig.3-11 Stress-strain curve for specimen B

(longitudinal)

Table 3-6 Typical tensile properties of steel sheet specimen B

Tensile axis	Young's modulus GPa	Yield strength MPa	Tensile strength MPa	Uniform elongation %	Total elongation %	Strain-rate sensitivity m	Anisotropy R
R.D.	202	368.54	391.98	13.219	14.133	0.0110	1.68
T.D.	203	365.38	390.56	12.500	13.260	0.0116	1.65
45°	204	370.24	396.24	12.734	13.563	0.0112	1.71
Average	203.3	368.60	393.76	12.797	13.630	0.0113	1.69

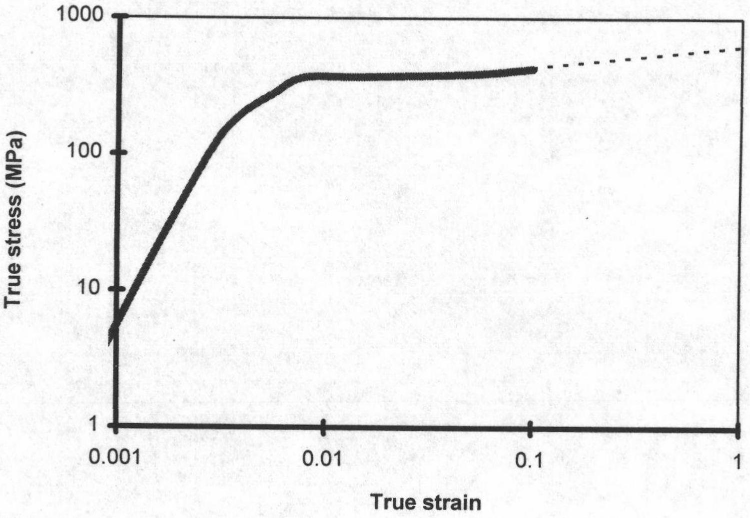

Fig.3-12 True stress-true strain curve for specimen B (longitudinal)

Table 3-7 Strain-hardening data of specimen B

Tensile axis	Strength coefficient K (MPa)	Strain-hardening exponent n
R.D.	622	0.104
T.D.	624	0.106
45°	617	0.102
Average	620	0.1035

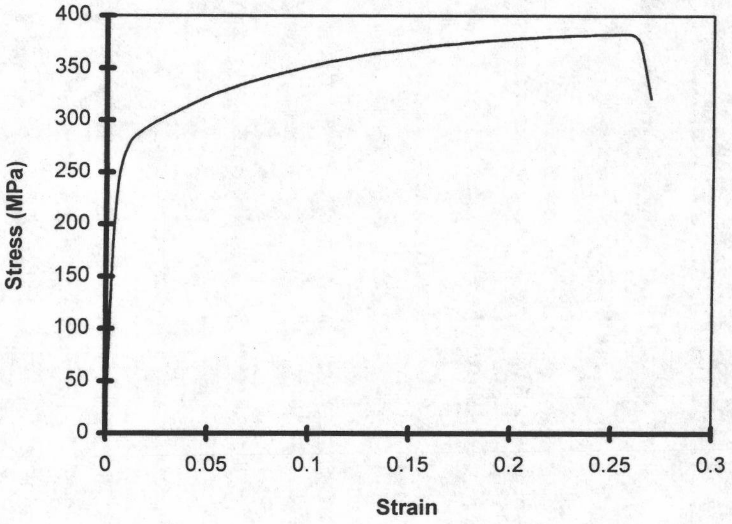

Fig.3-13 Stress-Strain curve for specimen C

(longitudinal)

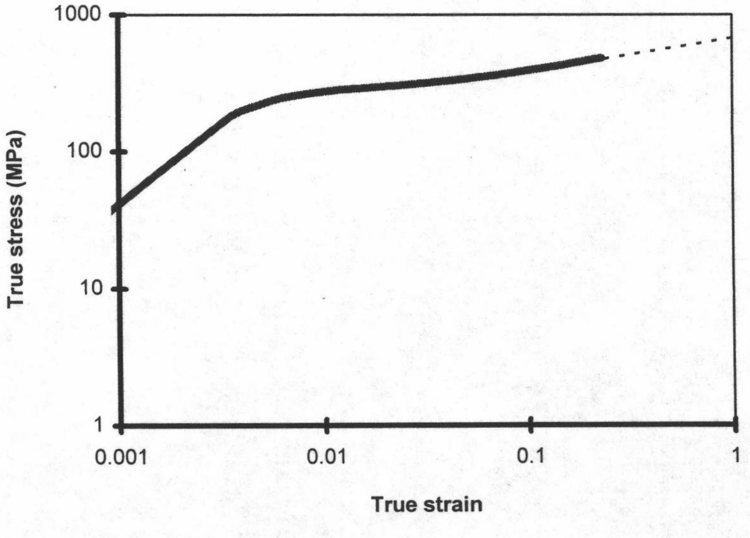

Fig.3-14 True stress-true strain curve for specimen C

(longitudinal)

Table 3-8 Typical tensile properties of steel sheet specimen C

Tensile axis	Young's modulus GPa	Yield strength MPa	Tensile strength MPa	Uniform elongation %	Total elongation %	Strain-rate sensitivity m	Anisotropy R
R.D.	201	268.26	382.51	25.959	27.500	0.0187	1.87
T.D.	197	269.13	382.24	25.429	27.093	0.0192	1.90
45°	198	264.67	380.54	25.775	27.293	0.0143	1.88
Average	200.8	266.68	381.46	25.735	27.295	0.0166	1.88

Table 3-9 Strain-hardening data of specimen C

Tensile axis	Strength coefficient K (MPa)	Strain-hardening exponent n
R.D.	702	0.26
T.D.	699	0.22
45°	701	0.24
Average	700.8	0.24

3.2 PLANE-STRAIN TENSILE TEST

3.2.1 SPECIMEN PREPARATION

The plane-strain tensile tests were performed in much the same way as the uniaxial tensile tests. In uniaxial tensile tests, the sample was strained in the region of drawing; i.e., the minor or width strain is negative. The test does not provide information on the response of sheet materials in the plane-strain state, in which the minor strain is zero. However, it can be modified to produce this strain state in part of the specimen. Increasing the width of the sample changes the strain state from one with a large negative minor strain component toward the plane-strain state. The specimen geometry that yielded the highest center strain at failure with a large region of plane-strain was prepared.

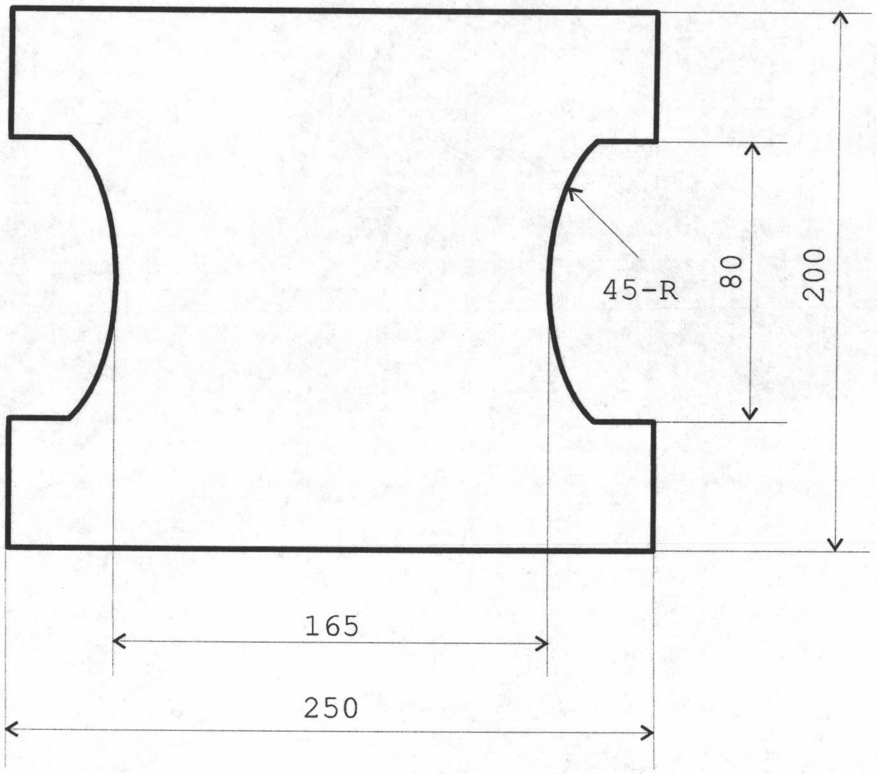

Unit: mm

Fig.3-15 Specimen for plane-strain tensile test

The specimens (shown in Fig.3-15) were prepared from the low-carbon steel sheet with the rolling direction parallel, at 45°, and normal to the load axis in order to check for anisotropic effects. All specimens were photogridded with 10 mm diameter circles. The crosshead displacement rates used in these tests were

10^{-3} mm/s and 5×10^{-3} mm/s, equivalent to average axial strain. Axial and transverse grid lengths were determined along the transverse center line from photographs using a Vernier caliper. The width of the specimen along the transverse center line was divided into three regions: the center section which had a strain state close to plane-strain and two edge sections near uniaxial tension. The plane-strain region, which was arbitrarily taken as the region where $|e_2/e_1|$ is less than 0.2, the outer part of the specimen deforms in a similar manner to a standard uniaxial tensile test specimen (R.H.Wagoner,1980). The load supported by the edge region was calculated using the strain distribution data and the strain work hardening curve obtained from uniaxial tensile tests. The error of this estimation should be small because the strain state was close to uniaxial tension. The average effective stress in the center(plane-strain) section was calculated after subtracting the estimated load supported by the edge(uniaxial) sections from the total recorded load. The remaining load was divided by the central region's cross sectional area to obtain the average axial stress. The results of tests exhibited that specimens used in this study contains plane-strain state approximately 80 pct of the width.

The test specimens were prepared by using a set of press die with the 0.005 mm clearance. The die used for preparing the specimens is shown in Fig.3-16 As the width of sample was wider than that of the standard specimen, special grips were prepared for holding the specimens in the plane-strain tensile tests. Fig.3-17 shows the sheet specimen gripping arrangement. The special grips and clippers are used to hold the specimen.

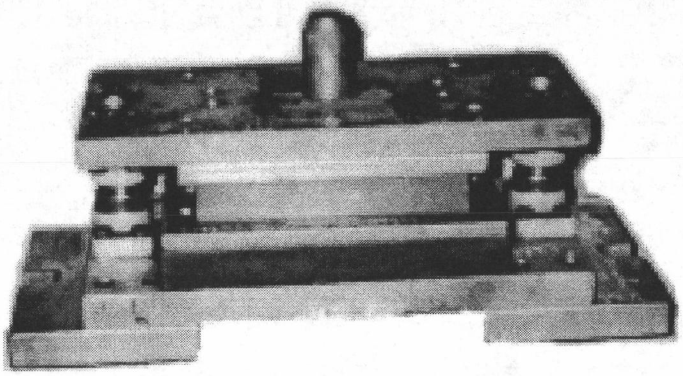

Fig.3-16 Die used for preparing the specimens in the plane-strain test

3.2.2 STRAIN-HARDENING CHARACTER

The experimental data of plane-strain tensile tests are shown below. True stress - true strain curves for each sample are shown on logarithmic coordinates. In the same way, there was no zero-zero starting point with logarithmic coordinates, the elastic region starts at some finite value. In these figures, the elastic zone near to the transition point and the plastic zone were

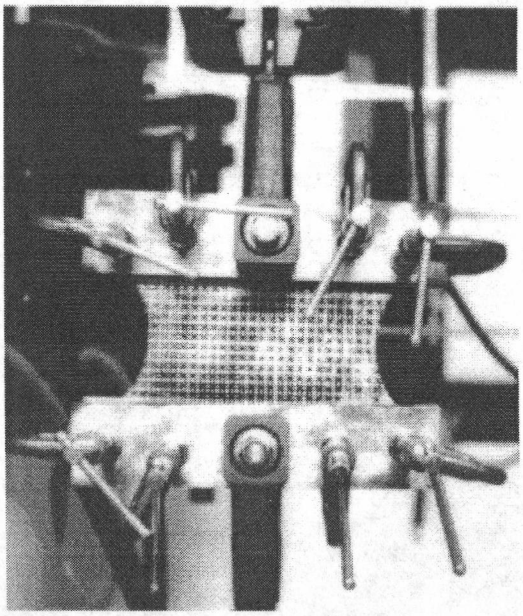

Fig.3-17 Grips and clippers

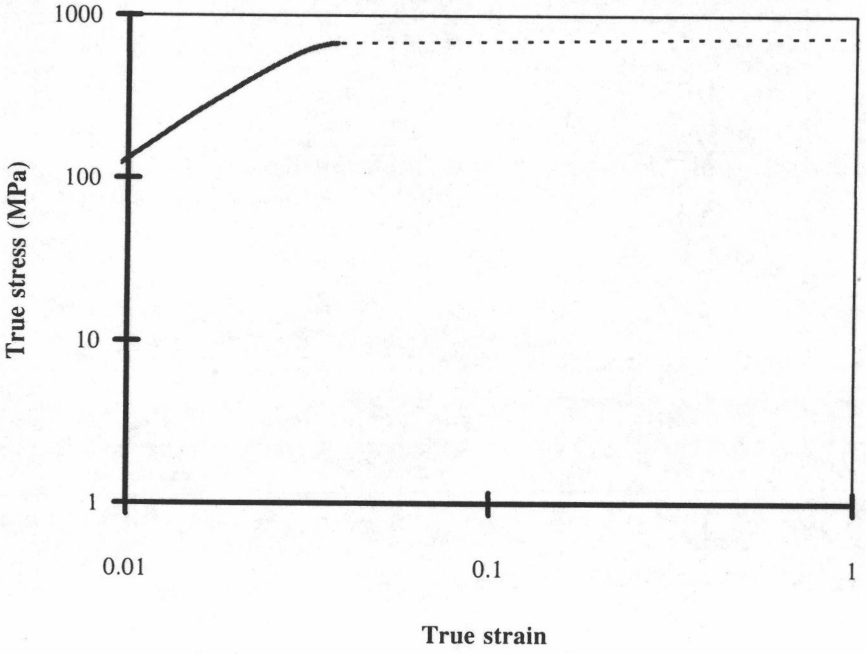

Fig.3-18 True stress-true strain curve for specimen A (longitudinal)

plotted on logarithmic coordinates. The slope of line for the plastic zone defined the strain-hardening exponent, n, and the intersection of this line with unit strain gave the stress value that defined the magnitude of K, strength coefficient.

Table 3-10 Strain-hardening data for specimen A

Tensile axis	Strength coefficient K (MPa)	Strain-hardening exponent n
R.D.	695	0.055
T.D.	698	0.057
45°	699	0.058
Average	697.8	0.057

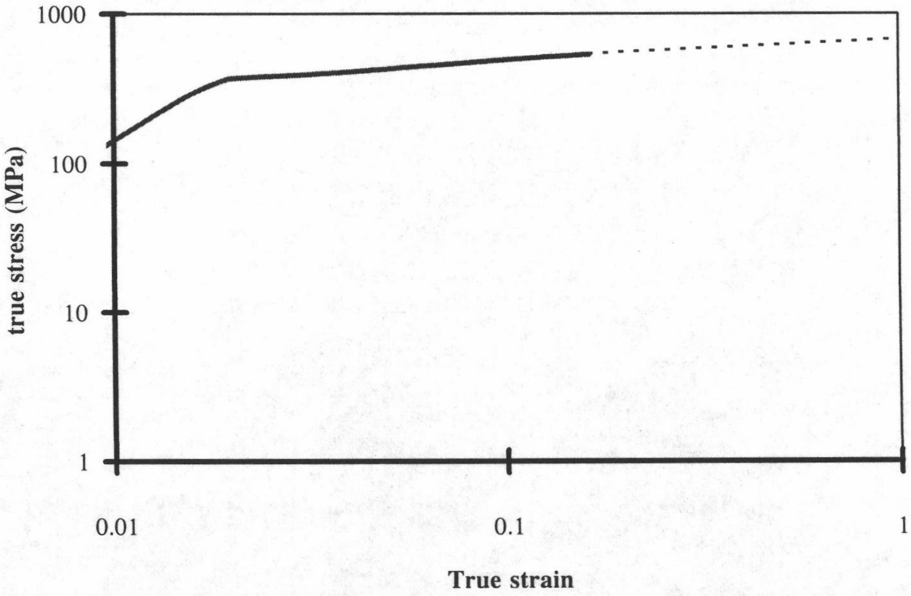

Fig.3-19 True stress-true strain curve for specimen B (longitudinal)

Table 3-11 Strain-hardening data for specimen B

Tensile axis	Strength coefficient K (MPa)	Strain-hardening exponent n
R.D.	719	0.112
T.D.	716	0.109
45°	723	0.110
Average	720.3	0.1103

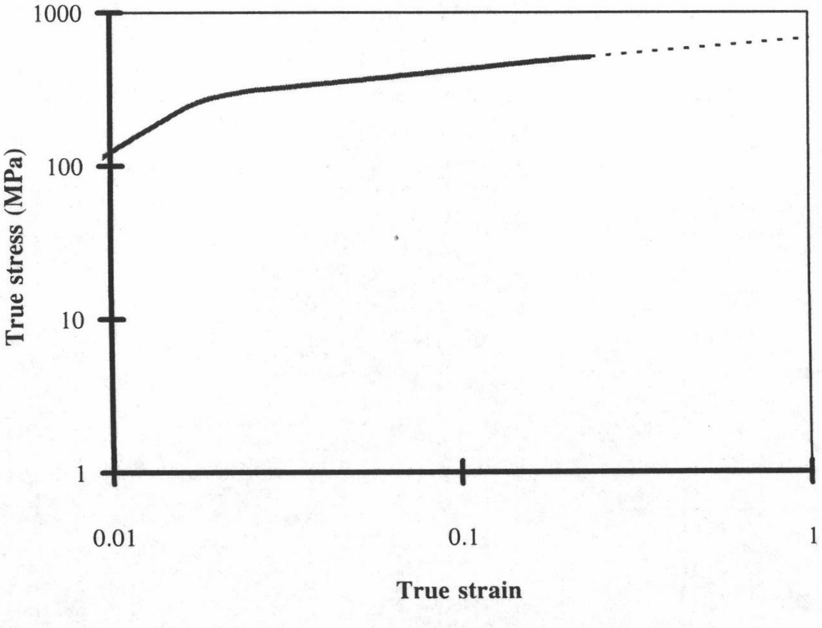

Fig.3-20 True stress-true strain curve for specimen C

(longitudinal)

Table 3-12 Strain-hardening data for specimen C

Tensile axis	Strength coefficient K (MPa)	Strain-hardening exponent n
R.D.	699	0.27
T.D.	695	0.25
45°	701	0.25
Average	699	0.255

3.2.3 FORMING LIMIT DIAGRAM

The forming limit diagram (left hand) was derived by measuring the grid of circles of diameter 10 mm printed on the surface of steel sheet before forming; during forming process these circles were distorted into ellipses. The principal strain can be determined by measuring the major diameter, d_1, and the minor diameter, d_2. By conversion, major strain $e_1 = (d_1 - d_0)/d_0$ and minor strain $e_2 = (d_2 - d_0)/d_0$ had been reported. These values at fracture give the "failure" condition, which strains in three circles from a failure were considered "safe". By plotting these measured strains it is possible to construct a forming limit diagram (FLD). The lowest value of e_1 occurs at plane-strain conditions (e_2=0).

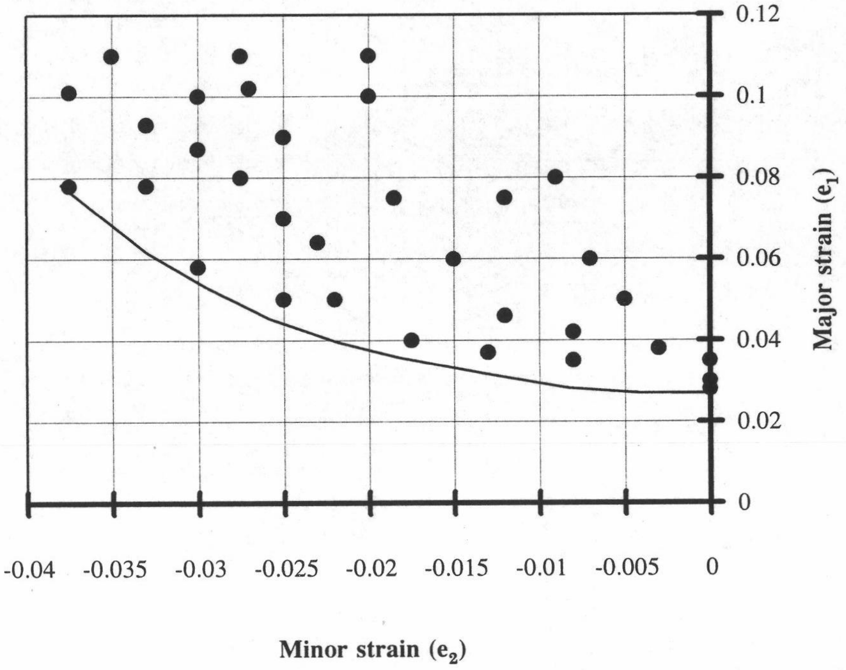

Fig.3-21 Forming limit diagram for specimen A

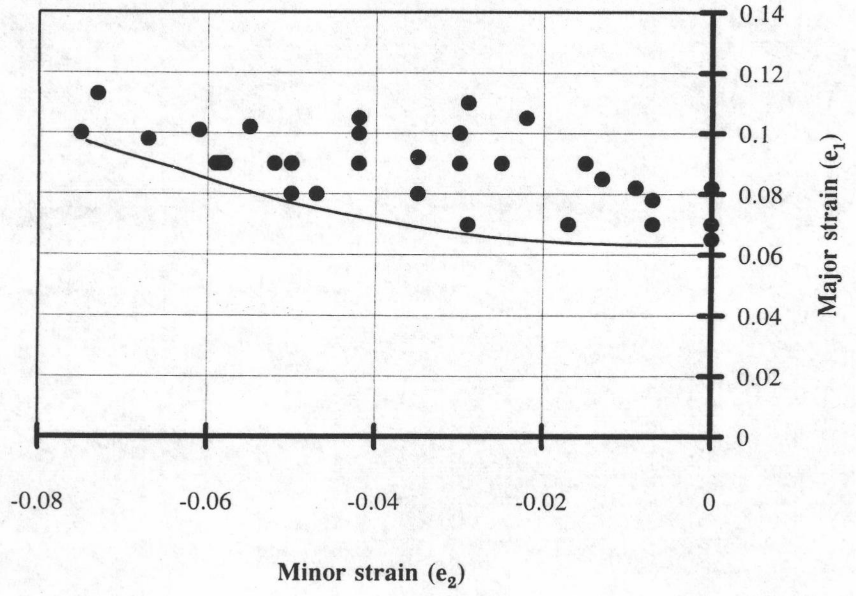

Fig.3-22 Forming limit diagram for specimen B

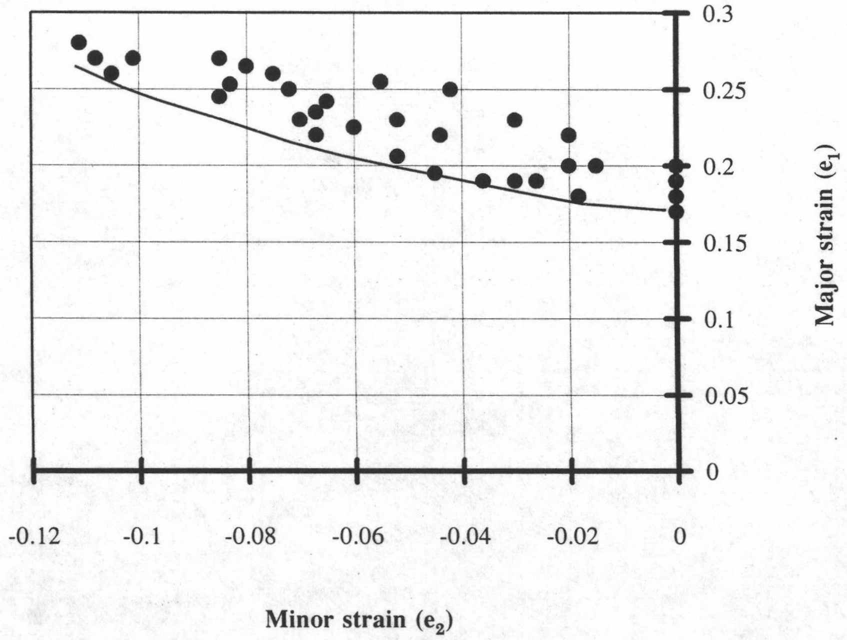

Fig.3-23 Forming limit diagram for specimen C

3.3 DRAWING TEST

3.3.1 LIMIT DRAWING RATIO TEST

A method was used for determining the limit drawing ratio by using blank with a diameter less than critical diameter in the standard test. The blanks were drawn to the maximum load, which usually occurs before 50% of the draw has occurred. The clamping force was then increased to prevent further drawing-in of the flange, and the load was increased to the point of fracture. The limit blanking diameter (LBD) was defined by:

$$\text{LBD} = \frac{\text{Fracture load } \times (\text{ blank diameter } - \text{ die diameter })}{\text{Maximum drawing load}} + \text{Die diameter}$$

The limit drawing ratio (LDR) was given by:

$$\text{LDR} = \frac{\text{LBD}}{\text{Punch diameter}}$$

In this study, the blank diameters used for cup drawing of every kind of steel sheet are shown in Table 3-13.

Table 3-13 Specimen for cup drawing tests

Specimen	Blank diameter (mm)
A	68±1
B	85±1
C	105±1

In this study, a set of die (shown in Fig.3-24) was used for carrying out the test on the universal tensile tester. A specimen was put on the surface of the die. A holder with screw was turned down to press the surface of specimen for preventing wrinkling, and the punch drawn the sample into the hole of die. When the load value recording from the tensile tester was at the maximum value, turned the holder down against to the die for locking the sample. The punch drawn the sample continuously to the point of fracture and the fracture load value was recorded. Then, the limit blanking diameter and the limit drawing ratio could be calculated by using the equation shown above.

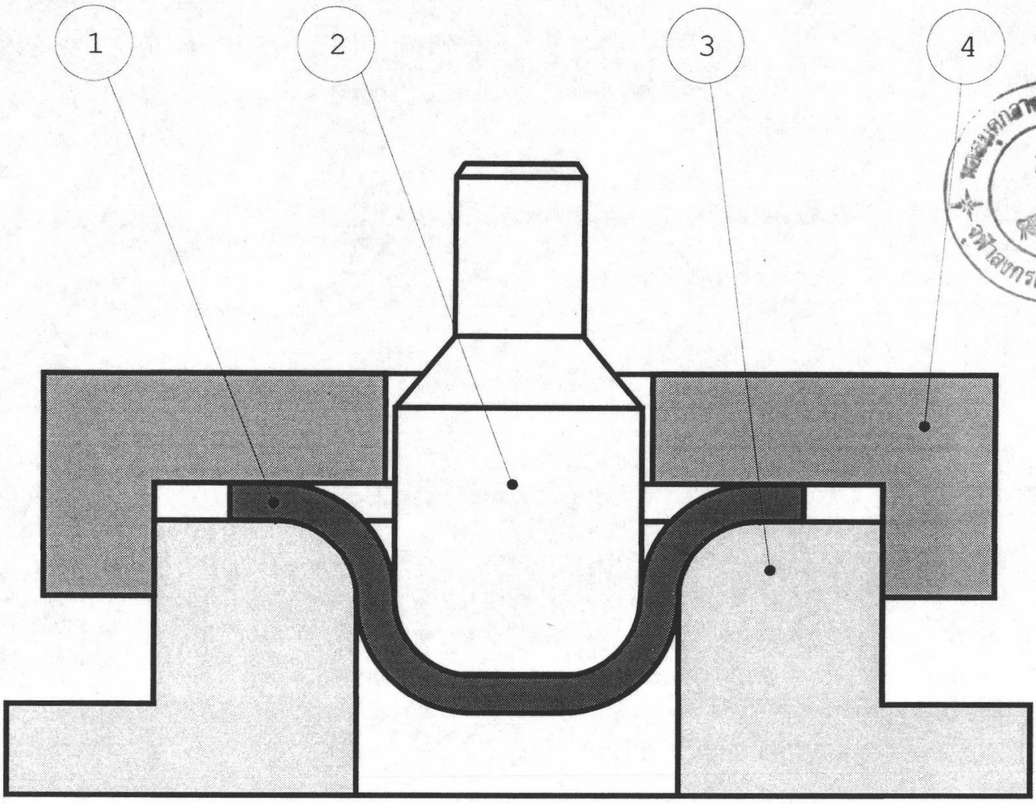

1-Specimen 2-Punch 3-Die 4-Holder

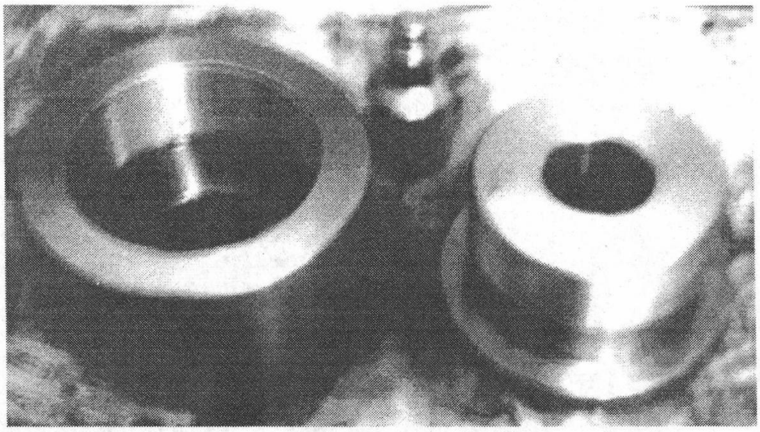

Fig.3-24 Drawing die used in test

3.3.2 RESULTS

The limit drawing test data are listed below, and these data are calculated by averaging the data attained from the tests for each specimen.

Table 3-14 Results of drawing tests

Specimen	Max. load (kg)	Frac.load (kg)	LBD (mm)	LDR
A	2783.5	3386.6	71.9	1.44
B	1492.5	1597.2	89.8	1.80
C	1600.0	1730.9	109.5	2.19